Available online at www.sciencedirect.com
ScienceDirect
Metabolism Clinical and Experimental 57 (2008) 1071 – 1077
Metabolism
Clinical and Experimental
www.metabolismjournal.com

Increased oxidative stress precedes the onset of high-fat diet–induced insulin resistance and obesity

Naoto Matsuzawa-Nagata[a,b], Toshinari Takamura[b,*], Hitoshi Ando[b], Seiji Nakamura[a,b], Seiichiro Kurita[b], Hirofumi Misu[b], Tsuguhito Ota[b], Masayoshi Yokoyama[b], Masao Honda[b], Ken-ichi Miyamoto[a], Shuichi Kaneko[b]

[a]*Department of Medicinal Informatics, Kanazawa University Graduate School of Medical Science, Kanazawa, Ishikawa 920-8641, Japan*
[b]*Department of Disease Control and Homeostasis, Kanazawa University Graduate School of Medical Science, Kanazawa, Ishikawa 920-8641, Japan*

Received 27 June 2007; accepted 28 March 2008

Abstract

Insulin resistance is a key pathophysiological feature of metabolic syndrome. However, the initial events triggering the development of insulin resistance and its causal relations with dysregulation of glucose and fatty acids metabolism remain unclear. We investigated biological pathways that have the potential to induce insulin resistance in mice fed a high-fat diet (HFD). We demonstrate that the pathways for reactive oxygen species (ROS) production and oxidative stress are coordinately up-regulated in both the liver and adipose tissue of mice fed an HFD before the onset of insulin resistance through discrete mechanism. In the liver, an HFD up-regulated genes involved in sterol regulatory element binding protein 1c–related fatty acid synthesis and peroxisome proliferator–activated receptor α–related fatty acid oxidation. In the adipose tissue, however, the HFD down-regulated genes involved in fatty acid synthesis and up-regulated nicotinamide adenine dinucleotide phosphate (NADPH) oxidase complex. Furthermore, increased ROS production preceded the elevation of tumor necrosis factor–α and free fatty acids in the plasma and liver. The ROS may be an initial key event triggering HFD-induced insulin resistance.

1. Introduction

Insulin resistance and obesity are generally brought about by an excessive nutrient condition attributable to an imbalance among energy intake, expenditure, and storage. Importantly, liver and adipose tissue jointly participate in maintaining glucose and lipid homeostasis through the secretion of various humoral factors and/or neural networks [1-3]. Previous studies have validated the presence of molecular signatures typical of the liver and adipose tissue in mouse models of obesity [4] and in mice fed a high-fat diet (HFD) [5]. It is believed that perturbations in these "intertissue communications" may be involved in the development of insulin resistance, obesity, and other features of metabolic syndrome [6]. It remains unclear, however, which factors alter communication among tissues and impair the ability of tissues to adapt to changing metabolic states.

To determine which initial events trigger the development of HFD-induced insulin resistance and obesity, we globally analyzed the biological pathways that are coordinately altered in both the liver and adipose tissue of mice fed an HFD. This was accomplished through the use of microarray and quantitative real-time polymerase chain reaction (PCR) analyses. We found that oxidative stress pathways, which are regulated through the balance of reactive oxygen species (ROS) production and antioxidant enzyme activity [7], are up-regulated in both tissues before the onset of insulin resistance and obesity induced by an HFD.

2. Materials and methods

2.1. Animals and experimental design

Male C57BL/6J mice were purchased from Charles River Laboratories Japan (Yokohama, Japan) at 6 weeks of age. After a 2-week acclimation period, the mice were divided randomly into 2 groups: (*a*) mice given a standard chow containing 5.9%

* Corresponding author. Tel.: +81 76 265 2233; fax: +81 76 234 4250.
E-mail address: ttakamura@m-kanazawa.jp (T. Takamura).

0026-0495/$ – see front matter © 2008 Elsevier Inc. All rights reserved.
doi:10.1016/j.metabol.2008.03.010

fat (in the form of soybean oil) by weight (control, n = 10) and (*b*) mice given an HFD containing 40% fat (in the form of cocoa butter) by weight (HFD, n = 10). Both diets used in this study were prepared by Oriental Yeast (Tokyo, Japan). The mice were housed in a room maintained at a controlled temperature (23°C ± 1°C) and a 12-hour light/12-hour dark cycle. In addition, animals were given free access to water and food. All animal procedures were in accordance with the Guidelines for the Care and Use of Laboratory Animals at the Takara-machi campus of Kanazawa University, Japan.

2.2. Glucose and insulin tolerance tests

For the oral glucose tolerance test (GTT), mice were fasted for 12 hours before glucose was administered at 1.5 g/kg body weight. For the insulin tolerance test (ITT), mice were injected intraperitoneally with insulin (0.5 U/kg body weight, Humulin R; Eli Lilly Japan, Kobe, Japan) after a 4-hour fast. Glucose values were measured in whole venous blood using a blood glucose monitoring system (FreeStyle; Kissei, Matsumoto, Japan) at 0, 15, 30, 60, and 120 minutes after the administration of either glucose or insulin.

2.3. Tissue preparation, blood sampling, and analysis

After a 12-hour fast, blood samples were obtained from the tail vein. Mice were then killed by cervical dislocation under diethyl ether anesthesia. The liver and adipose tissue (retroperitoneal fat) were immediately removed and weighed. A large portion of tissue was snap-frozen in liquid nitrogen for later RNA analysis. Enzymatic assays for total cholesterol, free fatty acids (FFAs), and triglycerides were performed using commercial kits purchased from Wako (Osaka, Japan). The plasma level of tumor necrosis factor (TNF) α was measured with a mouse TNF-α enzyme-linked immunosorbent assay kit (Pierce Biotechnology, Rockford, IL).

2.4. Measurement of hepatic lipid content

Hepatic lipids were extracted with chloroform-methanol (2:1) according to previously published methods [8]. The resulting extract was dissolved in water and subsequently analyzed for triglycerides, total cholesterol, and FFAs using commercial kits (Wako).

2.5. Measurement of oxidative stress in liver and adipose tissue

The concentration of proteins containing carbonyl groups in the liver and retroperitoneal fat (those that react with 2,4-dinitrophenylhydrazine to form the corresponding hydrazone) was determined spectrophotometrically according to commercial kit instructions (protein carbonyl assay kit; Cayman Chemical, Ann Arbor, MI).

2.6. RNA preparation for microarray and hybridization analysis

Total RNA was isolated from the frozen liver and retroperitoneal fat using a ToTALLY RNA kit (Applied Biosystems, Foster City, CA) and an RNeasy Lipid Tissue Mini kit (Qiagen, Germantown, MD), respectively. Each sample was prepared by pooling equal amounts of total RNA from 3 mice of the same experimental or control group. Three micrograms of total RNA was used for the synthesis of amino allyl antisense RNA with an Amino Allyl MessageAmp II aRNA kit (Applied Biosystems). These samples were then used for oligomicroarrays (AceGene Mouse 30K; DNA Chip Research, Yokohama, Japan). The microarray hybridization sample and reference antisense RNA were labeled with Cy5 and Cy3, respectively. Hybridization and washing were performed according to the manufacturer's instructions. The microarray was scanned using a G2505B microarray scanner (Agilent Technologies, Palo Alto, CA), and the image was analyzed using GenePix Pro 4.1 software (Axon Instruments, Union City, CA). An arbitrary cutoff signal value (<50) for both colors was used to filter genes with low expression values. Data were normalized (LOWESS method) using GeneSpring v7.2 software (Agilent Technologies). For pathway analysis, we used the GenMAPP and MAPPFinder software packages (http://www.genmapp.org) [9]. The GenMAPP program contains many pathway maps that can be associated with imported microarray data. The MAPPFinder program, which links gene expression data to the pathway maps, can calculate the *z* score (standardized difference score) and the percentage of genes measured that meet user-defined criteria (±20% in change-fold in our analysis). Using the *z* score and the percentage, the pathways were ranked by the relative amount of gene expression changes.

2.7. Quantitative real-time PCR

Total RNA (100 ng of the same sample used for microarray analysis) was reverse transcribed using random primers and SuperScript II reverse transcriptase (Invitrogen, Carlsbad, CA). The PCR was performed on an ABI PRISM 7900HT (Applied Biosystems). The specific PCR primers and TaqMan probes were obtained from Applied Biosystems. The PCR conditions were one cycle at 50°C for 2 minutes and 95°C for 10 minutes, followed by 40 cycles at 95°C for 15 seconds and 60°C for 1 minute.

2.8. Statistical analysis

All results are reported as means ± SD. Between-group differences in continuous variables were assessed by univariate analysis using Student *t* test. All calculations were performed with SPSS version 12.0 (SPSS, Chicago, IL).

3. Results

3.1. Effects of the HFD on metabolic parameters

As shown in Table 1, no differences were observed in any parameters between the HFD and control mice after 6 weeks of treatment. After 24 weeks, mice fed the HFD weighed significantly more and had more visceral fat compared with

Table 1
Clinical and biochemical parameters of mice fed the standard chow or HFD after 6 or 24 weeks

Diet type	6 wk		24 wk	
	Control	HFD	Control	HFD
Body weight (g)	25.1 ± 0.9	26.5 ± 1.4	29.0 ± 1.5	35.2 ± 3.8*
Liver weight (g)	1.11 ± 0.09	1.03 ± 0.12	1.28 ± 0.07	1.20 ± 0.23
Retroperitoneal fat pad weight (g)	0.07 ± 0.05	0.10 ± 0.08	0.24 ± 0.09	0.61 ± 0.17**
Plasma triglycerides (mg/dL)	69.1 ± 9.0	75.0 ± 18.9	41.5 ± 9.2	63.0 ± 15.0
Plasma total cholesterol (mg/dL)	85.0 ± 7.4	117.7 ± 37.0	84.6 ± 7.9	132.6 ± 26.1*
Plasma FFAs (mEq/L)	0.60 ± 0.16	0.61 ± 0.21	0.48 ± 0.09	0.54 ± 0.16
Plasma TNF-α (pg/mL)	<10	<10	ND	ND
Fasting plasma insulin (μU/mL)	14.6 ± 3.6	18.1 ± 7.6	15.7 ± 6.2	43.3 ± 14.3*
Hepatic triglycerides (μg/mg protein)	64.8 ± 23.2	73.8 ± 15.4	148.6 ± 46.7	143 ± 43.0
Hepatic total cholesterol (μg/mg protein)	43.0 ± 6.3	40.8 ± 6.0	34.3 ± 4.9	36.5 ± 4.5
Hepatic FFAs (μEq/mg protein)	46.7 ± 6.9	48.8 ± 3.6	53.1 ± 4.0	71.0 ± 7.6*

Values represent the means ± SD of 5 mice per group. ND indicates not determined.
Significantly different from control value: *$P < .05$; **$P < .01$.

control mice. Fasting plasma insulin levels were significantly higher in mice fed the HFD than in control mice. The HFD also induced the accumulation of FFAs in the liver after 24 weeks. These results suggest that mice fed the HFD maintained metabolic homeostasis up to 6 weeks, at which point obesity and insulin resistance developed.

3.2. Effects of the HFD on insulin sensitivity

To evaluate insulin sensitivity, GTT and ITT were conducted after 6 and 24 weeks of treatment in both groups (Fig. 1). Although there was no significant difference in the blood glucose level between the HFD and control mice at 6 weeks, the HFD mice exhibited impaired glucose tolerance (Fig. 1A) and insulin resistance (Fig. 1B) at 24 weeks. These results are consistent with the above observation that obesity, abdominal adiposity, and hyperinsulinemia were induced only after mice were fed the HFD for 24 weeks.

3.3. Fatty acid metabolism pathways are differentially regulated in liver and adipose tissue of mice fed the HFD

We compared liver and adipose tissue gene expression data between mice fed the HFD and control mice after

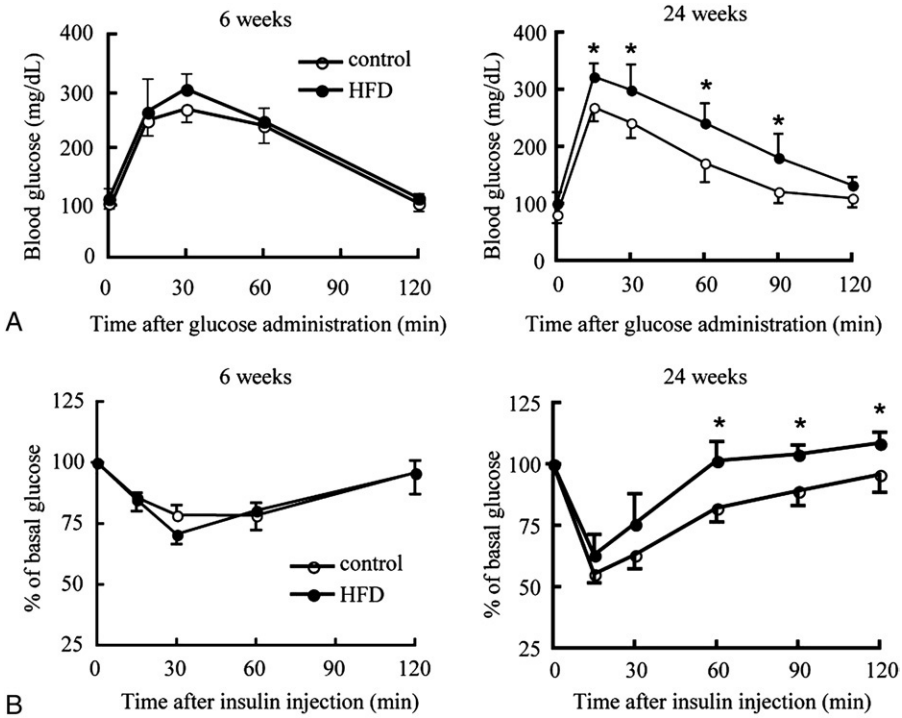

Fig. 1. Evaluation of glucose tolerance and insulin sensitivity. The GTT (A) and ITT (B) after 6 or 24 weeks of standard chow or the HFD. Values represent the means ± SD for 5 mice. *$P < .05$ vs the control group.

6 weeks of treatment to identify pathways with the potential to induce insulin resistance (Table 2). The gene expression levels of various metabolic pathways were already altered at 6 weeks. In particular, pathways for sterol regulatory element binding protein 1c–related fatty acid synthesis (Fig. 2 and Supplementary Fig. 1A) and peroxisome proliferator–activated receptor (PPAR) α–related fatty acid oxidation were up-regulated in the liver of the HFD mice. In contrast, the pathway for fatty acid synthesis was down-regulated in the adipose tissue (Supplementary Fig. 1B). Such compensatory alterations in the expression of genes that regulate fatty acid metabolism seem to help maintain plasma and hepatic levels of FFAs, which have been considered to be a causal factor for insulin resistance [10,11]. In the current study, these levels were similar between the HFD mice and control mice at 6 weeks (Table 1).

3.4. Oxidative stress pathways are coordinately up-regulated in both liver and adipose tissue of mice fed the HFD

In contrast to the pathways for fatty acid metabolism, oxidative stress pathways were coordinately up-regulated in both the liver and adipose tissue (Table 2 and Supplementary Fig. 1C, D). The oxidative stress pathway is composed of genes for ROS production, stress signaling, and antioxidant enzymes. Reactive oxygen species are radical forms of oxygen that can arise from several biochemical reactions: (1) loading of excessive electrons in the respiratory chain by increased mitochondrial fatty acid β-oxidation [12], (2) peroxisomal fatty acid β-oxidation by acyl–coenzyme A oxidase (Acox) [13], (3) microsomal fatty acid ω-oxidaiton by cytochrome P450 2E1 (CYP2E1) [14], and (4) reduction of oxygen by the nicotinamide adenine dinucleotide phosphate (NADPH) oxidase (Nox) complex [15].

To determine the sources of ROS in the liver and adipose tissue of mice fed the HFD, we examined the messenger RNA (mRNA) expression levels of genes involved in ROS production through the use of quantitative real-time PCR (Fig. 2). In the liver of mice fed an HFD for 6 weeks, the expression levels of genes encoding key regulators of mitochondrial fatty acid β-oxidation, including PPARα, carnitine palmitoyltransferase 1a (CPT-1a), Acox1, and CYP2E1, were significantly up-regulated (1.6-, 2.0-, 1.5-, and 1.5-fold, respectively) compared with control mice, whereas the expression levels of Nox2, Nox4, and the Nox complex components $p22^{phox}$ and $p47^{phox}$ were similar between HFD mice and control mice. In the adipose tissue of mice fed an HFD for 6 weeks, gene expression levels of Acox1, CYP2E1, Nox4, and $p22^{phox}$ were significantly up-regulated (1.6-, 1.4-, 2.3-, and 1.6-fold, respectively) compared with control mice; in contrast to the liver, the adipose tissue did not show up-regulated expression of the genes for PPARα and CPT-1a. These results suggest that the source of ROS may differ according to the specific tissue, such that an HFD may induce ROS production in distinctly different manners in the liver and adipose tissue. An HFD may induce ROS production through fatty acid oxidation in the mitochondria of the liver but via Nox in the adipose tissue.

Table 2
Biological pathways of liver or adipose tissue genes regulated by the HFD after 6 weeks

Pathway name	Number of genes changed	Number of genes measured	z score	permuted P value
Liver				
Up-regulated				
Cholesterol biosynthesis	10	15	4.61	<.001
Fatty acid synthesis	9	14	4.23	<.001
Oxidative stress	16	38	3.52	.001
Glucocorticoid mineralocorticoid metabolism	7	12	3.39	.006
Statin pathway	9	19	3.06	.005
Glycolysis and gluconeogenesis	14	41	2.37	.018
Fatty acid beta oxidation	10	27	2.30	.021
Down-regulated				
Electron transport chain (= respiratory chain)	28	82	4.77	<.001
ACE-inhibitor pathway	5	8	3.72	.003
Adipose tissue				
Up-regulated				
TGF Beta signaling pathway	27	50	3.645	.001
Complement and coagulation cascades	29	59	3.149	.001
Adipogenesis	51	129	2.638	.014
Oxidative stress	18	38	2.287	.026
Smooth muscle contraction	61	157	2.282	.024
Inflammatory response pathway	18	40	2.018	.037
Down-regulated				
Focal adhesion	74	189	3.50	<.001
Glycolysis and gluconeogenesis	21	41	3.35	<.001
Electron transport chain (= respiratory chain)	35	82	3.01	.002
Krebs-TCA cycle	14	29	2.46	.020
Fatty acid synthesis	8	14	2.45	.029
Pentose phosphate pathway	5	8	2.19	.038

Pathway analysis was performed using MAPPFinder 2.0 and the Mm-std 20051114.gdb database. The criteria for genes with significantly increased or decreased expression were change-fold (ratio to control) >20% (ie, >1.20 or <0.83). For each pathway, the number of genes that meet the criteria for a significant increase or decrease was determined. This number was compared with the number of pathway genes detected by microarray analysis. These values were used to calculate the *z* score and the permuted *P* value. Pathways indicated by arrows were coordinately regulated between the liver and adipose tissue (retroperitoneal fat). On the other hand, pathways for fatty acid synthesis and glycolysis and gluconeogenesis were up-regulated in the liver (highlighted in dark grey) and down-regulated in adipose tissue (highlighted in light grey).

Oxidative stress is regulated by the balance between ROS production and antioxidant enzyme activity [7]. Consequently, we determined the expression levels of the genes for glutathione peroxidase (Gpx) and Mn–superoxide dismutase, both of which reduce ROS and lipid peroxides, resulting in decreased oxidative stress (Fig. 2). The

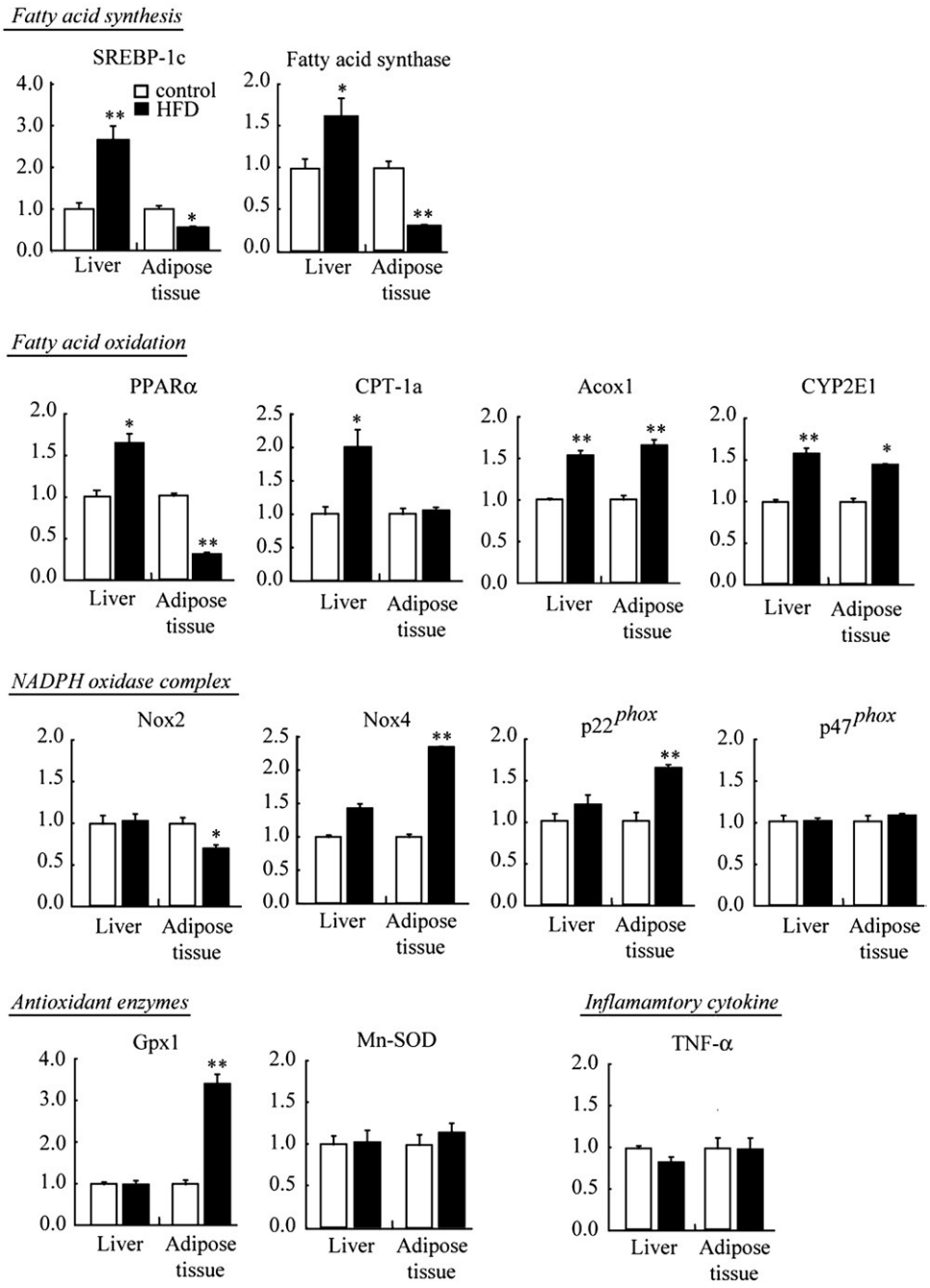

Fig. 2. Quantitative real-time PCR for representative genes involved in fatty acid metabolism and oxidative stress. The mRNA levels of sterol regulatory element binding protein 1c, fatty acid synthase, PPARα, CPT-1a, Acox1, CYP2E1, Nox2, Nox4, $p22^{phox}$, $p47^{phox}$, Gpx1, Mn–superoxide dismutase, and TNF-α in the liver or retroperitoneal fat of mice fed standard chow (n = 3) or the HFD (n = 3) were quantified using real-time PCR after 6 weeks of feeding. The RNA samples for real-time PCR were the same as those for the microarray analysis. Gene expression levels were normalized to 18S ribosomal RNA. The degree of change in gene expression is based on the mean expression level of control mice. Values represent the means ± SD for 3 mice. $^{*}P < .05$ and $^{**}P < .01$ vs the control mice.

expression level of the Gpx1 gene was significantly up-regulated (3.4-fold) in the adipose tissue, but not in the liver, of mice fed the HFD compared with control mice. The insufficient up-regulation of antioxidant enzymes may therefore cause more oxidative stress in the liver than in the adipose tissue.

The proinflammatory cytokine TNF-α, which is elevated in obese rodents and humans, is also an important contributor to the development of insulin resistance [16]. However, the mRNA expression level of TNF-α in the liver and adipose tissue of mice fed the HFD for 6 weeks was similar to that of control mice (Fig. 2). Furthermore, the plasma level of TNF-α was below the detection limit of the enzyme-linked immunosorbent assay (<10 pg/mL) in both groups. These results suggest that the up-regulation of genes for ROS production, rather than the elevation of

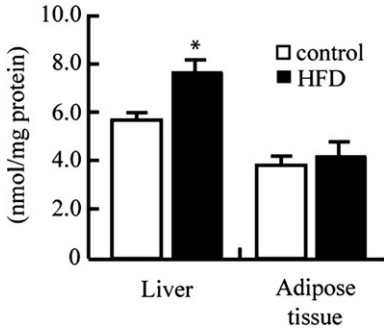

Fig. 3. Measurement of protein carbonyl levels in the liver and adipose tissue. Protein carbonyl concentration was analyzed as a marker for oxidative stress in the liver and retroperitoneal fat. Values represent the means ± SD for 5 mice. *$P < .05$ vs the control mice.

TNF-α, may be an early event triggering insulin resistance in mice fed an HFD.

3.5. Evaluation of oxidative stress in the liver and adipose tissue of mice fed the HFD

To confirm whether high fat intake increases oxidative stress, we measured the protein carbonyl level (marker for cumulative oxidative stress) in the liver and adipose tissue. As expected, the protein carbonyl level was elevated by 35% in the liver but was not altered in the adipose tissue of mice fed the HFD compared with control mice at 6 weeks (Fig. 3). The up-regulation of antioxidant enzymes (ie, Gpx1) in the adipose tissue may compensate for the increase of ROS, lowering oxidative stress.

4. Discussion

Reactive oxygen species production is one of many factors that have been suggested to play a role in the development of insulin resistance, based on the following evidence: (1) high doses of hydrogen peroxide [17] and reagents that accumulate ROS [18] can induce insulin resistance in 3T3-L1 adipocytes, and (2) increased markers of oxidative stress were observed in obese humans [19] and rodents [17,20]. It remains unclear, however, whether increased ROS production causes insulin resistance in vivo. In this study, we demonstrated that the up-regulation of genes responsible for ROS production occurs in both the liver and adipose tissue before the onset of insulin resistance and obesity in mice fed an HFD.

In our dietary model of insulin resistance, the mRNA up-regulation of genes for fatty acid oxidation was observed in the liver. Previous studies have also shown that fatty acid oxidation was increased in the liver to compensate for high fat intake [21]. In addition, pathways involved in the mitochondrial respiratory chain were coordinately down-regulated in both the liver and adipose tissue of mice fed the HFD. These results are consistent with previous reports in skeletal muscle of both humans and mice [22]. High mitochondrial β-oxidation rates seem to help metabolize excess FFAs, although large amounts of electrons entering the respiratory chain may cause abnormal reduction of oxygen. An influx of electrons may then lead to increased mitochondrial ROS production. This suggests that impaired respiratory chain function may cause increased mitochondrial ROS production. Furthermore, we speculate that the down-regulation of the respiratory chain may lead to an influx of FFAs to intracellular peroxisomes and microsomes instead of to mitochondria, resulting in further generation of ROS by Acox and CYP2E1, genes up-regulated in both liver and adipose tissue in this study.

The Nox complex may be a major source of ROS production in adipose tissue but not in liver. Furukawa et al [17] reported that the mRNA expression of Nox2 and its subunits $p22^{phox}$, $p47^{phox}$, and $p67^{phox}$ was significantly up-regulated in the adipose tissue of obese KKAy mice compared with lean C57BL/6J mice. In the present study, however, the HFD up-regulated only Nox4 and $p22^{phox}$ expression in adipose tissue. This discrepancy may be attributed to the difference between genetically and HFD-induced obese models. Given that complexes of Nox4 with $p22^{phox}$ increase in the kidney of diabetic rats [23], excessive nutrients (eg, high fat intake) may also induce ROS production via the Nox4/$p22^{phox}$ complex.

It is striking that increased ROS production preceded the elevated levels of TNF-α and FFAs in the plasma and liver. Although TNF-α and FFAs are thought to cause insulin resistance, our results raise the possibility that ROS trigger the development of insulin resistance, resulting in abdominal obesity and elevated TNF-α and FFAs. In summary, the HFD induced oxidative stress, potentially through the up-regulated expression of genes for ROS production, in the liver and adipose tissue. In addition, these changes occurred before the onset of insulin resistance and obesity. Sources of ROS induced by an HFD may differ between the liver and adipose tissue. These findings suggest that ROS production may be the initial event triggering HFD-induced insulin resistance and therefore may be an attractive therapeutic target for preventing insulin resistance and obesity caused by an HFD.

Acknowledgment

We thank A Katayama and M Nakamura for technical assistance.

Appendix A. Supplementary data

Supplementary data associated with this article can be found, in the online version, at doi:10.1016/j.metabol.2008.03.010.

References

[1] Yamauchi T, Kamon J, Minokoshi Y, Ito Y, Waki H, Uchida S, et al. Adiponectin stimulates glucose utilization and fatty-acid

oxidation by activating AMP-activated protein kinase. Nat Med 2002;8: 1288-95.
[2] Watanabe M, Houten SM, Mataki C, Christoffolete MA, Kim BW, Sato H, et al. Bile acids induce energy expenditure by promoting intracellular thyroid hormone activation. Nature 2006;439:484-9.
[3] Uno K, Katagiri H, Yamada T, Ishigaki Y, Ogihara T, Imai J, et al. Neuronal pathway from the liver modulates energy expenditure and systemic insulin sensitivity. Science 2006;312:1656-9.
[4] Lan H, Rabaglia ME, Stoehr JP, Nadler ST, Schueler KL, Zou F, et al. Gene expression profiles of nondiabetic and diabetic obese mice suggest a role of hepatic lipogenic capacity in diabetes susceptibility. Diabetes 2003;52:688-700.
[5] Gregoire FM, Zhang Q, Smith SJ, Tong C, Ross D, Lopez H, et al. Diet-induced obesity and hepatic gene expression alterations in C57BL/6J and ICAM-1-deficient mice. Am J Physiol Endocrinol Metab 2002;282:E703-13.
[6] Herman MA, Kahn BB. Glucose transport and sensing in the maintenance of glucose homeostasis and metabolic harmony. J Clin Invest 2006;116:1767-75.
[7] Nordberg J, Arner ES. Reactive oxygen species, antioxidants, and the mammalian thioredoxin system. Free Radic Biol Med 2001;31: 1287-312.
[8] Folch J, Lees M, Sloane Stanley GH. A simple method for the isolation and purification of total lipids from animal tissues. J Biol Chem 1957; 226:497-509.
[9] Doniger SW, Salomonis N, Dahlquist KD, Vranizan K, Lawlor SC, Conklin BR. MAPPFinder: using Gene Ontology and GenMAPP to create a global gene-expression profile from microarray data. Genome Biol 2003;4:R7.
[10] Boden G. Role of fatty acids in the pathogenesis of insulin resistance and NIDDM. Diabetes 1997;46:3-10.
[11] Boden G, She P, Mozzoli M, Cheung P, Gumireddy K, Reddy P, et al. Free fatty acids produce insulin resistance and activate the proinflammatory nuclear factor–kappaB pathway in rat liver. Diabetes 2005; 54:3458-65.
[12] St-Pierre J, Buckingham JA, Roebuck SJ, Brand MD. Topology of superoxide production from different sites in the mitochondrial electron transport chain. J Biol Chem 2002;277:44784-90.
[13] Osmundsen H, Bremer J, Pedersen JI. Metabolic aspects of peroxisomal beta-oxidation. Biochim Biophys Acta 1991;1085: 141-58.
[14] Chitturi S, Farrell GC. Etiopathogenesis of nonalcoholic steatohepatitis. Semin Liver Dis 2001;21:27-41.
[15] Krieger-Brauer HI, Kather H. Human fat cells possess a plasma membrane–bound H2O2-generating system that is activated by insulin via a mechanism bypassing the receptor kinase. J Clin Invest 1992;89: 1006-13.
[16] Hotamisligil GS, Shargill NS, Spiegelman BM. Adipose expression of tumor necrosis factor–alpha: direct role in obesity-linked insulin resistance. Science 1993;259:87-91.
[17] Furukawa S, Fujita T, Shimabukuro M, Iwaki M, Yamada Y, Nakajima Y, et al. Increased oxidative stress in obesity and its impact on metabolic syndrome. J Clin Invest 2004;114:1752-61.
[18] Lin Y, Berg AH, Iyengar P, Lam TK, Giacca A, Combs TP, et al. The hyperglycemia-induced inflammatory response in adipocytes: the role of reactive oxygen species. J Biol Chem 2005;280:4617-26.
[19] Urakawa H, Katsuki A, Sumida Y, Gabazza EC, Murashima S, Morioka K, et al. Oxidative stress is associated with adiposity and insulin resistance in men. J Clin Endocrinol Metab 2003;88:4673-6.
[20] Diniz YS, Rocha KK, Souza GA, Galhardi CM, Ebaid GM, Rodrigues HG, et al. Effects of *N*-acetylcysteine on sucrose-rich diet–induced hyperglycaemia, dyslipidemia and oxidative stress in rats. Eur J Pharmacol 2006;543:151-7.
[21] Akbiyik F, Cinar K, Demirpence E, Ozsullu T, Tunca R, Haziroglu R, et al. Ligand-induced expression of peroxisome proliferator–activated receptor alpha and activation of fatty acid oxidation enzymes in fatty liver. Eur J Clin Invest 2004;34:429-35.
[22] Sparks LM, Xie H, Koza RA, Mynatt R, Hulver MW, Bray GA, et al. A high-fat diet coordinately downregulates genes required for mitochondrial oxidative phosphorylation in skeletal muscle. Diabetes 2005;54: 1926-33.
[23] Etoh T, Inoguchi T, Kakimoto M, Sonoda N, Kobayashi K, Kuroda J, et al. Increased expression of NAD(P)H oxidase subunits, NOX4 and p22phox, in the kidney of streptozotocin-induced diabetic rats and its reversibity by interventive insulin treatment. Diabetologia 2003;46: 1428-37.